

# The Influence of Blade Structure Optimization on the Hydraulic Performance of Vane Pump

Jianqiang Sun<sup>1,2,\*</sup>, Sheng Li<sup>1,2</sup>, Hao Wang<sup>1,2</sup>

<sup>1</sup>Department of Mechatronic Engineering, Southwest Petroleum University, Chengdu 610500, PR China

<sup>2</sup>Oil and gas equipment technology Sharing and Service Platform of Sichuan Province, Chengdu 610500, PR China

\*Corresponding author: Jianqiang Sun

**Abstract:** Vane pump has the problems of low pressure reduction efficiency and easy to be stuck at the bottom of the well. In order to solve this problem, the annular pressure reduction downhole tool of vane pump based on eddy current principle is adopted. On the basis of introducing the principle of eddy current hydraulic pressure reduction technology, this paper studies the influence of blade number, blade outlet angle, blade chord height and blade thickness on tool characteristics. The results show that the tool head increases with the increase of blade number, increases first and then decreases with the increase of blade outlet angle, and decreases first and then stabilizes with the increase of blade wall thickness and chord height. The tool efficiency increases with the increase of blade number, decreases with the increase of blade chord height, and decreases with the increase of blade outlet angle to a certain value, which is less sensitive to blade wall thickness. The research results have important guiding significance for the design and structural optimization of blade annular pressure reducing tools.

**Keywords:** Vortex Principle; Annular Pressure Drop; Structural Optimization; Vane Pump.

## 1. Introduction

The vane pump uses the eddy current principle to pump the bottom hole, reduce the density of the drilling fluid and cause the decrease of the bottom hole pressure difference, reduce the pressure holding effect of the drilling fluid on the bottom hole and improve the penetration rate. Because of its large head and high efficiency, the vane pump has a wide application prospect in the downhole annulus pressure reduction tool. However, the vane pump is directly connected to the drill bit, which limits the rotation speed of the vane pump, so the pressure reduction effect is limited. At the same time, it is placed at the bottom of the well, and it is easy to be stuck by the falling block or collapsed cuttings of the upper wellbore, which restricts the development and application of the technology to a certain extent.

The technology of annulus pressure drop is hollow sphere double gradient or riser dilution double gradient drilling [1]. The tool designed by Li Jun [1] to reduce the equivalent circulation density can achieve safe and efficient drilling for lower bottom pressure. Liu Yong wang [2] et al. proposed a downhole annulus drilling fluid depressurization device and method based on drill string vibration. Using drill string vibration as an energy source, it not only reduces the harm of drill string vibration, but also reduces the bottom hole drilling fluid pressure and improves rock breaking efficiency. The working theory and optimization design of jet mill bit proposed by Cao Tong et al. [4] proposed the parameter optimization method of maximum rock carrying hydraulic efficiency and maximum rock clearing jet water power. Li Gensheng [5] -[8] designed the hydraulic pulse cavitation jet generator, and carried out the field test. The test results show that the hydraulic cavitation jet generator can improve the penetration rate by more than 20 %.

However, the above technical solutions have the problems of high cost and low efficiency. Based on the principle of eddy current, this paper establishes a numerical model of the annular pressure drop tool of the vane pump, and studies the

influence of different geometric parameters on the pressure drop effect of the tool. The research results have certain guiding significance for the design and structural optimization of the annular pressure drop tool of the vane pump.

## 2. Tool Structure and Working Principle

### 2.1. Tool structure parameters

The structure of the vane pump annular pressure lowering downhole tool using the eddy current effect is shown in Figure 1. The structural parameters of the tool include blade thickness, blade number, blade chord length, and blade inlet angle as shown in Figure 2. The main design parameters and the geometric parameters of the model are shown in Table 1.

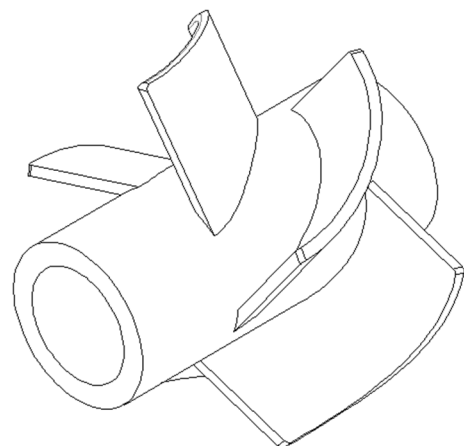


Figure 1. Three-dimensional model of blade pump

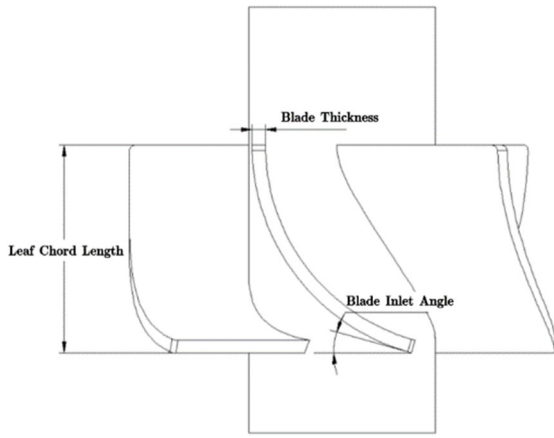


Figure 2. Vane pump parameter diagram

Table 1. Parameters of vane pump

Technical Parameter	Value
Number of blades Z	5
Thickness b/mm	5
$\alpha/(\circ)$	15
h/mm	78
Q/(m <sup>3</sup> /min)	2
n/rpm	812
Fluid medium	Water

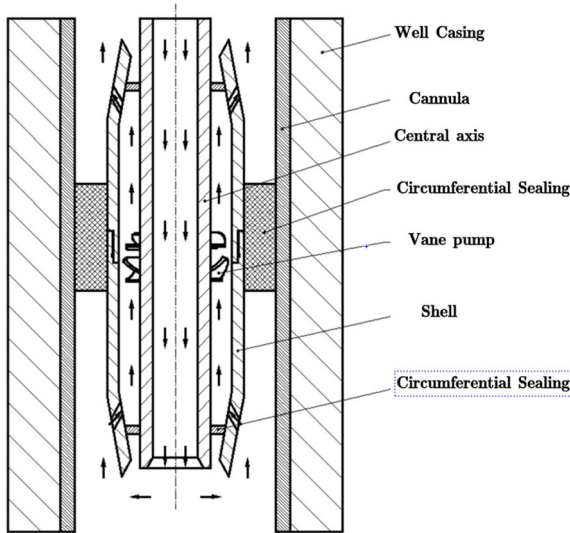


Figure 3. Tool schematics

## 2.2. Tool principal

The pressure reduction of the vane pump is based on the principle of eddy current. As shown in figure 3, the vane pump is installed on the drive center shaft and rotates with the rotation of the drive center shaft. The drilling fluid flows out from the inside of the drive center shaft and enters the external annulus. Because the rotary motion of the vane pump causes the drilling fluid to produce a strong vortex, which has a suction effect on the bottom hole, so that the drilling fluid enters the casing of the vane pump from the lower opening of the external annulus and flows out from the upper opening, and then enters the external annulus again, resulting in a decrease in the bottom hole pressure difference, reducing the pressure holding effect of the drilling fluid on the bottom hole and increasing the penetration rate.

## 3. Numerical Method

### 3.1. Continuity equation

$$\frac{\partial}{\partial t}(\rho_g \alpha_g A) + \frac{\partial}{\partial z}(\rho_g \alpha_g v_g A) = q_g \quad (1)$$

$$\frac{\partial}{\partial t}(\rho_1 \alpha_1 A) + \frac{\partial}{\partial z}(\rho_1 \alpha_1 v_1 A) = 0 \quad (2)$$

$$\frac{\partial}{\partial t}(\rho_s \alpha_s A) + \frac{\partial}{\partial z}(\rho_s \alpha_s v_s A) = q_s \quad (3)$$

In the formula : A is the area of annular flow channel, m<sup>2</sup> ;  $\rho_g$ ,  $\rho_1$  and  $\rho_s$  are the density of intrusive gas, drilling fluid and cuttings respectively, kg/m<sup>3</sup>.  $\alpha_g$ ,  $\alpha_1$  and  $\alpha_s$  are the volume fraction of intrusive gas, drilling fluid and cuttings respectively, dimensionless.  $v_g$ ,  $v_1$ ,  $v_s$  are the flow velocity of intrusive gas, drilling fluid and cuttings, respectively, m/s;  $q_g$  is the intrusion gas velocity per unit thickness, kg/(s·m);  $q_s$  is the production rate of rock debris per unit thickness, kg/(s·m) [9].

### 3.2. Turbulent Flow Model

$$\frac{\partial(\rho k)}{\partial t} + \frac{\partial(\rho k u_i)}{\partial x_i} = \frac{\partial}{\partial x_i} \left[ \left( \mu + \frac{\mu_t}{\sigma_k} \right) \frac{\partial k}{\partial x_i} \right] + G_k + G_b - \rho \varepsilon - Y_M + S_k \quad (4)$$

$$\frac{\partial(\rho \varepsilon)}{\partial t} + \frac{\partial(\rho \varepsilon u_i)}{\partial x_i} = \frac{\partial}{\partial x_i} \left[ \left( \mu + \frac{\mu_t}{\sigma_\varepsilon} \right) \frac{\partial \varepsilon}{\partial x_i} \right] + G_{\varepsilon k} - C_{2\varepsilon} \rho \frac{\varepsilon^2}{k} + S_\varepsilon \quad (5)$$

$$\mu_t = \rho C_\mu \frac{k^2}{\varepsilon} \quad (6)$$

Where  $k$  is turbulent kinetic energy, J ;  $\mu_t$  is turbulent viscosity, Pa s ;  $\varepsilon$  is the turbulent dissipation rate, W/m<sup>3</sup> ;  $G_k$  is the production term of turbulent kinetic energy caused by average velocity ;  $G_b$  is the generation term of turbulent kinetic energy  $k$  caused by buoyancy ; the contribution of  $Y_M$  to the fluctuating expansion in compressible turbulence ;  $S_k$ ,  $S_\varepsilon$  are self-defined dimensionless parameters ;  $C_{1\varepsilon} = 1.44$ ,  $C_{2\varepsilon} = 1.92$ ,  $C_\mu = 0.09$  are empirical constants [10].

### 3.3. Model validation and mesh independence analysis

According to the model of 600ZLB-70 axial flow pump, the main design parameters are as follows : speed  $n_a = 730$ rpm, flow  $Q_a = 910$ L/S, head  $H_a = 8.1$ m, fluid medium is water. The geometric parameters of the model are shown in Table 2. The error between the calculated head of the axial flow pump of 9.3m and the theoretical head of 8.1m is 14.4 %, as shown in figure 5.

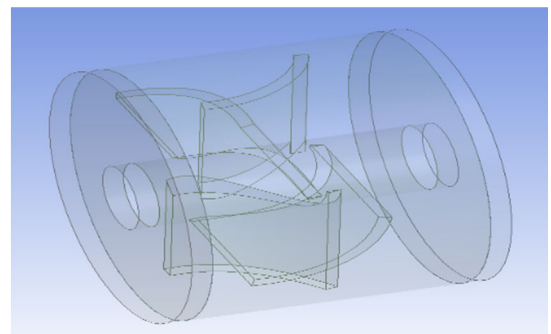
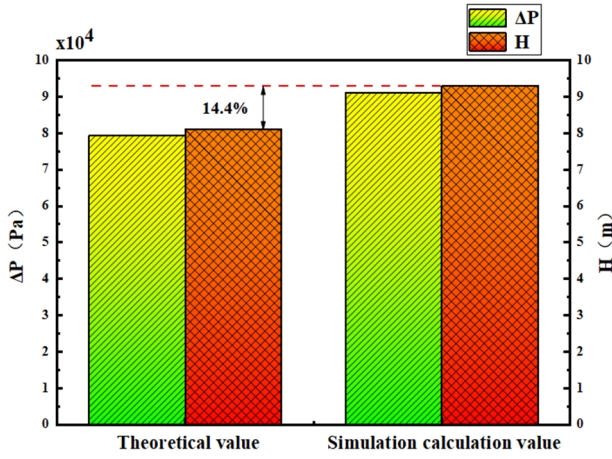


Figure 4. Three-dimensional diagram of 600ZLB-70 model

**Table 2.** Main geometric parameters of 600ZLB-70 axial flow pump

Technical Parameter	Value
D1/mm	550
D2/mm	140
ha/mm	200
L/mm	400



**Figure 5.** Model validation diagram

Refinement of the mesh is an effective way to improve the calculation accuracy of the structural model. However, it is followed by a balance between computational efficiency and accuracy and computational time. Most of the computers hardware and software performance have certain limitations. It is necessary to select the appropriate mesh generation method and the number of meshes, and use the lower computational cost to obtain the ideal results as far as possible. In principle, the finer the mesh is, the higher the accuracy of the solution is. However, in the design and application of practical engineering, the sharp increase in the number of grids will lead to a significant increase in the time cost of calculation, and when the number of grids reaches a certain number of stars, the improvement of calculation accuracy is not obvious. Therefore, in engineering applications, the grid that meets the calculation accuracy should be selected. To distinguish the importance of different parts of the model, the key parts and key nodes need to improve the calculation accuracy, and the refined Ager can be selected, while the parts far away from the constraints and loads or the parts less affected by the constraints and loads can be appropriately selected. Rough grids are used for discretization, and limited resources and time are used for key parts and nodes of the structure [11].

The quantity and quality of the grid will have a great influence on the calculation results. The grid independence verification in this paper is under the same model, and the head generated by the model under the same working conditions is used as the evaluation index. By increasing or decreasing the number of grids, a total of 5 grid schemes are generated as shown, and the total number of grids is 688300, 789628, 1147234, 1209970, 1624199. As shown in Figure 6, with the increasing number of grids, the maximum head is

4.98 m, the minimum is 4.82m, and the change amplitude is 3%, which satisfies the grid independence. Therefore, we choose the total number of grids 688300 for simulation.

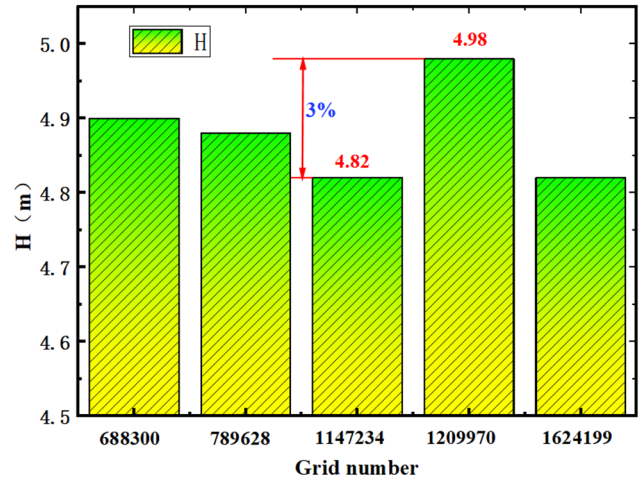


**Figure 6.** Grid independence verification

## 4. Parameter Analysis of Single Blade

### 4.1. Influence of blade number on hydraulic performance of vane pump

For the blade annular pressure reducing downhole tool, the blade is the core of the tool, and the change of its structural parameters will affect the hydraulic performance of the tool. Therefore, the change of the number of blades will cause the change of the working performance of the tool. In order to study the influence of the number of blades on the working performance of the tool, the simulation calculation is carried out under the condition of 4,5,6,7 and 8 blades respectively. The pressure nephograms of 4,5,6,7 and 8 blades are shown in Fig.7a-e, and the changes of head and tool efficiency under different blade numbers are obtained.

It can be seen from Fig.8 that when the number of leaves  $n$  is 4, the head  $H$  of the tool is 2.5m. When the number of leaves  $n$  increases to 8, the head  $H$  of the tool is 4.4m. With the increase of the number of leaves  $n$ , the head  $H$  generated by the tool will increase, and it is linear with the change of the number of leaves  $n$ . It can be seen from Fig.9 that when the number of leaves  $n$  is 4, the efficiency  $\eta$  of the tool is 71%. When the number of leaves  $n$  is 8, the efficiency  $\eta$  of the tool is 94%. With the increase of the number of leaves  $n$ , the efficiency  $\eta$  of the tool will also increase, showing a linear relationship with the number of tools  $n$ . The number of blades  $n$  is 10, which is 78% higher than the number of blades  $n$  is 4 head  $H$ ; the efficiency  $\eta$  is increased by 32%. This is because the flow of the fluid in the blade flow channel is more disordered, and the number of blades is increased. The narrowing of the flow channel between adjacent blades can make the water flow more stable and eliminate the circulation effect, making the fluid flow more uniform. The hydraulic loss in the blade flow channel is reduced, and the hydraulic efficiency of the tool is improved.

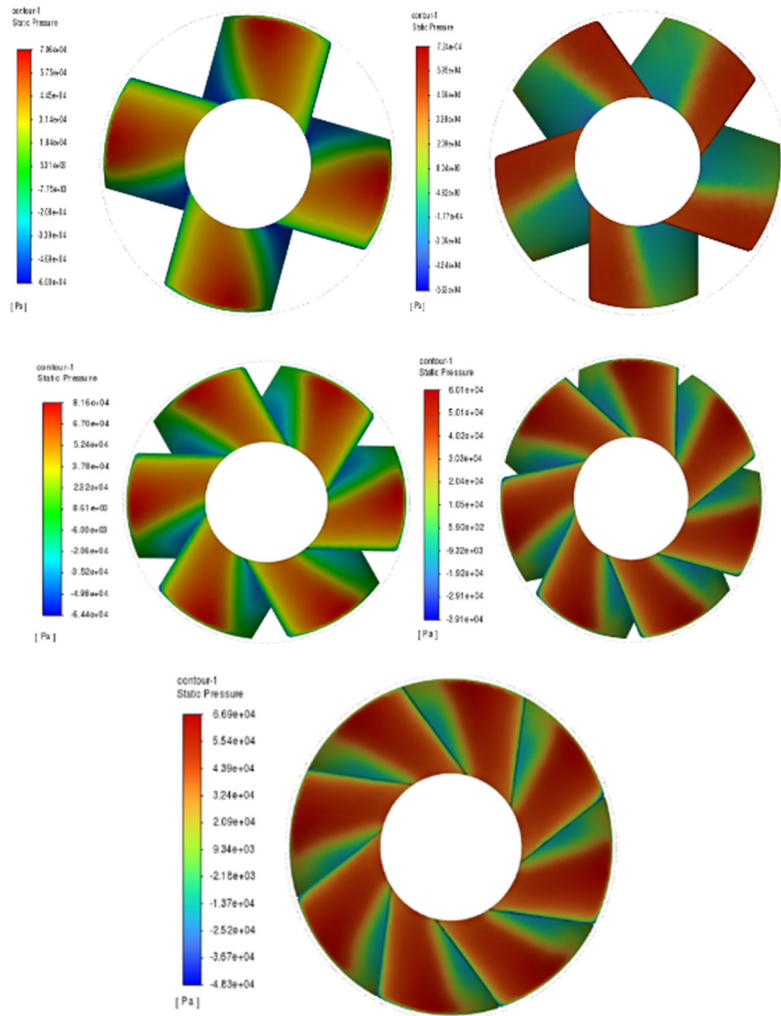


Figure 7. Pressure cloud diagram of different leaf number

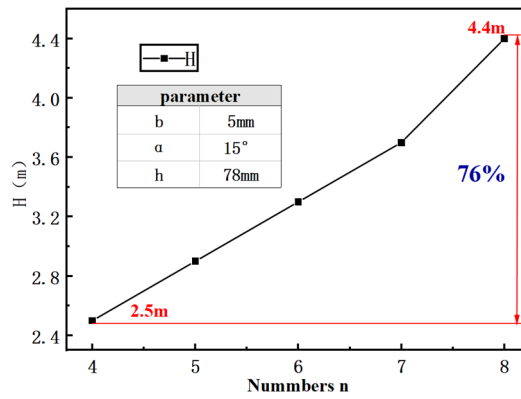


Figure 8. Effect of leaf number on head

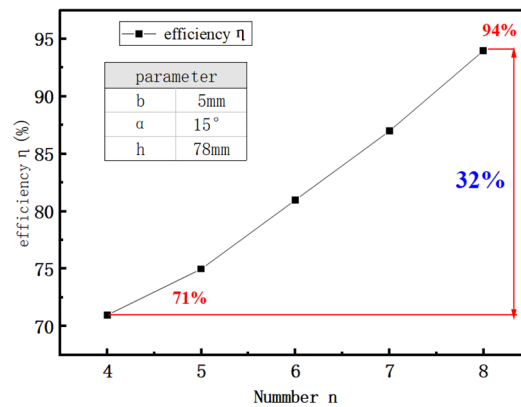


Figure 9. The influence diagram of the number of leaves on efficiency

## 4.2. Influence of blade outlet angle on hydraulic performance of vane pump

For the blade annular pressure reducing downhole tool, the blade is the core of the tool, and the change of its structural parameters will affect the hydraulic performance of the tool. Therefore, the change of the blade outlet angle will cause the

change of the working performance of the tool. In order to study the influence of the number of blades on the working performance of the tool, the simulation calculation is carried out under the condition of the blade outlet angle of 20°, 25°, 30° and 35° respectively. The pressure cloud diagram of the blade outlet angle of 20°, 25°, 30° and 35° is shown in Figure 10a-d, and the changes of head and tool efficiency under different blade outlet angles are obtained.

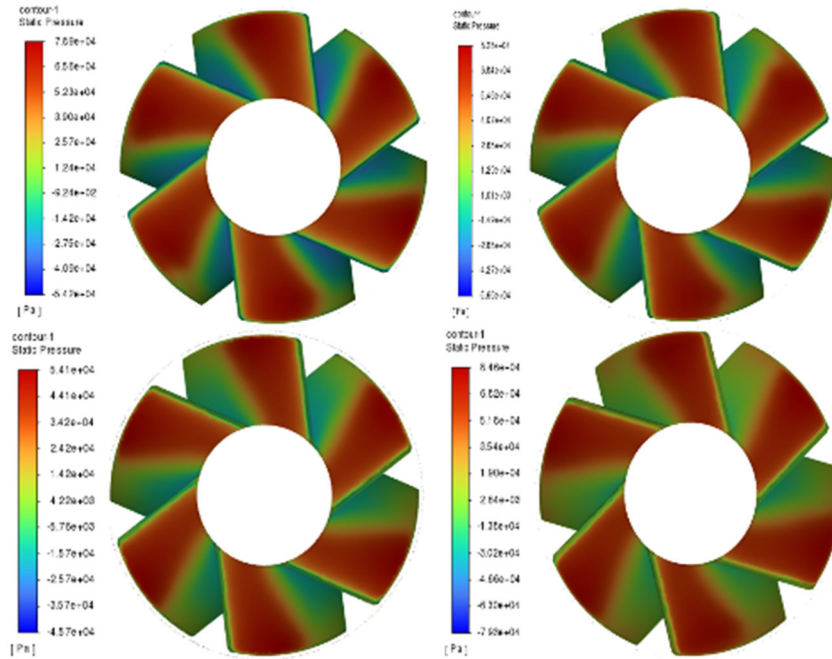


Figure 10. Pressure cloud diagram of vane pump under different blade outlet angles

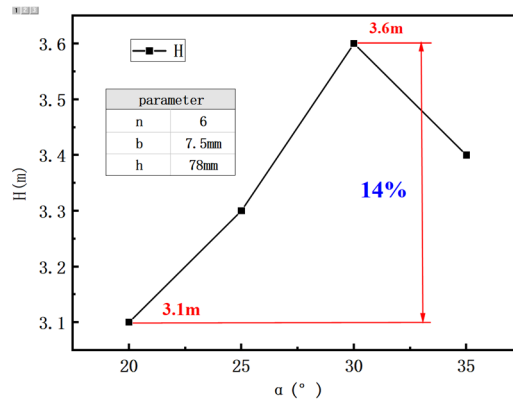


Figure 11. Shadow of blade outlet angle on head

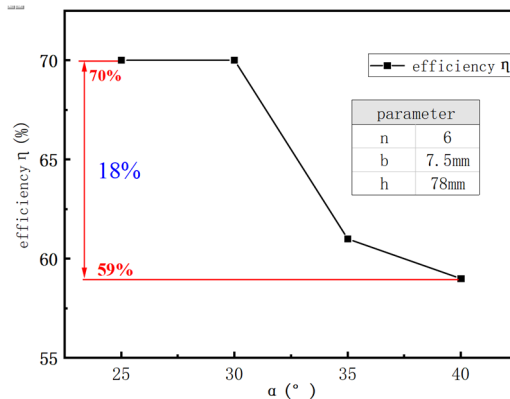


Figure 12. Effect of blade outlet angle on efficiency

From Figure 11, it can be seen that when the blade outlet angle  $\alpha$  is 20°, the head  $H$  of the tool is 3.1 m. When the blade

outlet angle  $\alpha$  is  $25^\circ$ , the head  $H$  of the tool is 3.3m. When the blade outlet angle  $\alpha$  is  $30^\circ$ , the head  $H$  of the tool is 3.6m. When the blade outlet angle  $\alpha$  increases to  $35^\circ$ , the head  $H$  of the tool decreases to 3.4 m. With the increase of the blade outlet angle  $\alpha$ , the head  $H$  generated by the tool will increase first, and it is linear with the change of the blade outlet angle  $\alpha$ . Then the head  $H$  of the tool decreases with the continuous increase of the blade wall thickness  $b$ . When the blade outlet angle  $\alpha$  is  $30^\circ$ , the head  $H$  is increased by 24% compared with that when the blade outlet angle  $\alpha$  is  $20^\circ$ . This is because from the perspective of the change of the blade outlet angle  $\alpha$ , increasing the blade outlet angle  $\alpha$  effectively slows down the growth rate of the flow channel area, thereby suppressing the boundary layer separation phenomenon in the blade flow channel. This improves the flow condition of the fluid in the flow channel to a certain extent and reduces the flow loss of the vane pump. However, when the blade outlet angle  $\alpha$  increases excessively, the fluid at the outlet of the flow channel can not change the direction of motion under the action of centrifugal force, and a violent collision occurs near the tongue, so that the backflow phenomenon occurs near the corresponding outlet of the flow channel. Affect the hydraulic performance of the pump.

The blade with large blade wall thickness  $b$  has a small flow section area due to serious extrusion, and the backflow and secondary backflow at the inlet and outlet of the blade are more serious, and the hydraulic loss is larger, so the head  $H$  of the tool is reduced. However, when the blade wall thickness  $b$  reaches 7.5mm, the blade wall thickness  $b$  has little effect on the head  $H$  of the tool. From Figure 12, it can be seen that when the blade wall thickness  $b$  is 2.5mm and 5mm, the efficiency of the tool is 70%. When the blade wall thickness

$b$  increases to 7.5mm, the efficiency  $\eta$  of the tool decreases to 69%. When the blade wall thickness  $b$  continues to increase to 10.0mm and 12.5mm, the efficiency  $\eta$  of the tool is stable to 69%. With the increase of the blade wall thickness  $b$ , the efficiency  $\eta$  generated by the tool decreases first and then tends to be stable. When the blade wall thickness  $b$  is 5mm, the efficiency  $\eta$  is 1.4% lower than that when the blade wall thickness  $b$  is 7.5mm. Although there is a change, the amplitude of the change is very small. This shows that because of the increase of blade wall thickness  $b$ , the blade conductivity and energy conversion ability are enhanced, but the crowding between the blades is also enhanced, which will also lead to the increase of hydraulic loss between the guide vanes, so the efficiency of the tool  $\eta$  changes little.

### 4.3. Influence of blade wall thickness on hydraulic performance of vane pump

Blade wall thickness is an important structural parameter of vane pump. The change of blade wall thickness will affect the hydraulic loss of vane pump, because the change of blade wall thickness will cause the change of blade pressure surface, fluid conductivity and energy conversion ability. In order to study the influence of blade wall thickness on the working performance of the tool, the simulation calculation is carried out under the condition of blade wall thickness of 2.5mm, 5.0mm, 7.5mm, 10.0mm and 12.5mm respectively. The pressure of blade wall thickness of 2.5mm, 5.0mm, 7.5mm, 10.0mm and 12.5mm is shown in figure 13, and the changes of head and tool efficiency under different blade wall thickness are obtained.

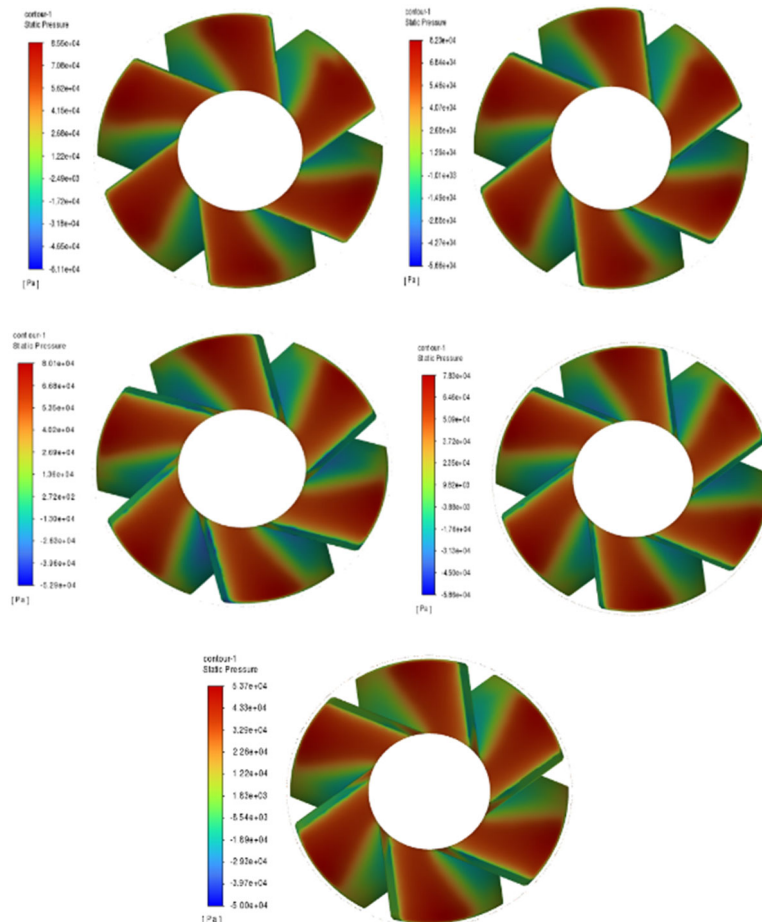


Figure 13 Pressure cloud of vane pump under different blade wall thickness

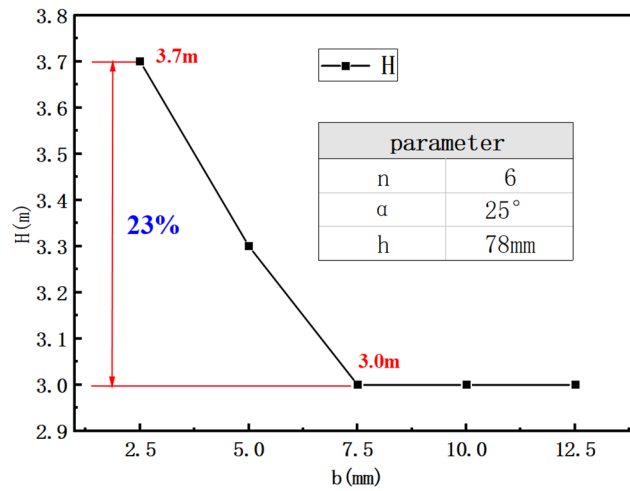


Figure 14. Effect of blade wall thickness on head

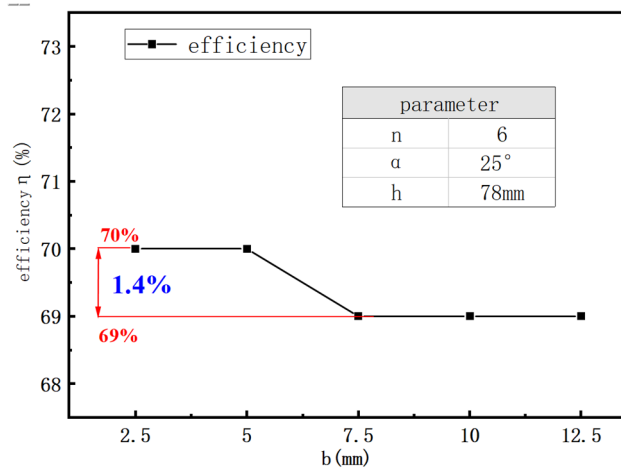


Figure 15. Effect of blade wall thickness on efficiency

It can be seen from Fig.14 that when the blade wall thickness  $b$  is 2.5mm, the head  $H$  of the tool is 3.7m. When the blade wall thickness  $b$  increases to 7.5mm, the head  $H$  of the tool decreases to 3.0m. When the blade wall thickness  $b$  continues to increase to 10.0mm and 12.5mm, the head  $H$  of the tool is stable to 3.0m. With the increase of the blade wall thickness  $b$ , the head  $H$  generated by the tool will increase first, and there is a linear relationship with the change of the blade wall thickness  $b$ . Then the head  $H$  of the tool tends to be stable with the continuous increase of the blade wall thickness  $b$ . When the blade wall thickness  $b$  is 2.5mm, the head  $H$  is reduced by 23% compared with that when the blade wall thickness  $b$  is 7.5mm. This is because the blade with a large blade wall thickness  $b$  has a small cross-sectional area due to serious crowding, and the backflow and secondary backflow at the inlet and outlet of the blade are more serious, and the hydraulic loss is larger. Therefore, the head  $H$  of the tool is reduced. However, when the blade wall thickness  $b$  reaches 7.5mm, the blade wall thickness  $b$  has little effect on the head  $H$  of the tool. It can be seen from Fig.15 that when the blade wall thickness  $b$  is 2.5mm and 5mm, the efficiency of the tool is 70%. When the blade wall thickness  $b$  increases to 7.5mm, the efficiency of the tool decreases to 69%. When the blade wall thickness  $b$  continues to increase to 10.0mm and 12.5mm, the efficiency of the tool is stable to 69%. With the increase of blade wall thickness  $b$ , the efficiency  $\eta$

generated by the tool decreases first and then tends to be stable. When the blade wall thickness  $b$  is 5mm, the efficiency  $\eta$  is 1.4% lower than that when the blade wall thickness  $b$  is 7.5mm. Although there is a change, the amplitude of the change is very small. This shows that because of the increase of blade wall thickness  $b$ , the blade conductivity and energy conversion ability are enhanced, but the crowding between the blades is also enhanced, which will also lead to the increase of hydraulic loss between the guide vanes, so the efficiency of the tool  $\eta$  changes little.

#### 4.4. Influence of blade chord height on hydraulic performance of vane pump

As an important structural parameter of vane pump, the change of blade chord height will affect the hydraulic loss of vane pump, because the change of blade chord height will cause the change of blade pressure surface, fluid conductivity and energy conversion ability. In order to study the influence of blade chord height on the working performance of the tool, the simulation calculation is carried out under the condition that the blade chord height is 78mm, 88mm, 98mm and 108mm respectively. The pressure contours of the blade chord height of 78mm, 88mm, 98mm and 108mm are shown in Figure 16, and the changes of head and tool efficiency under different blade chord heights are obtained.

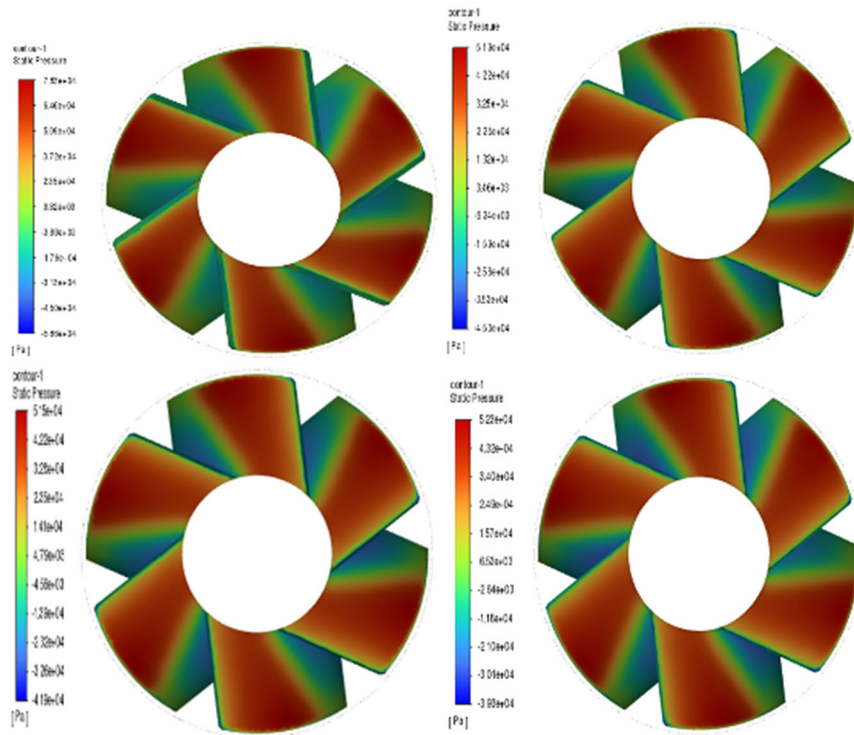


Figure 16. Pressure cloud diagram of vane pump under different blade chord height

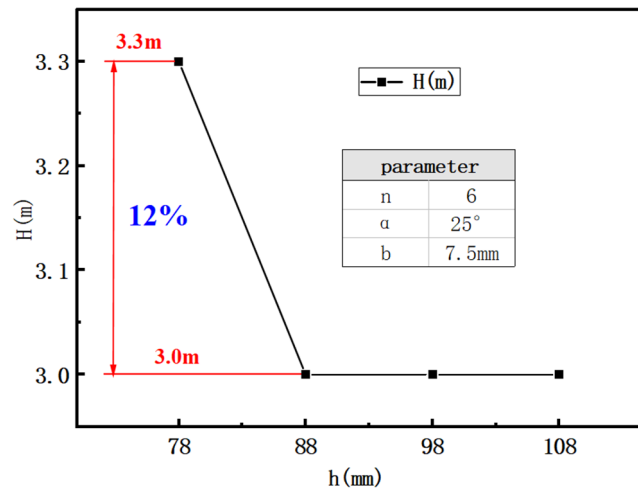


Figure 17. Effect of blade chord height on head

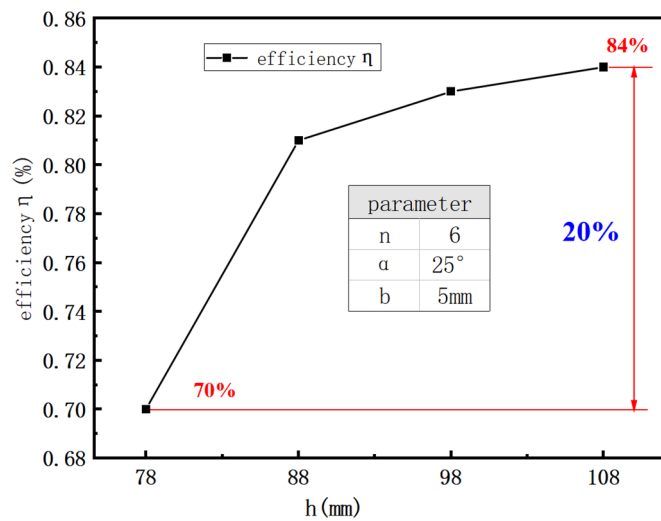


Figure 18. Effect of blade chord height on efficiency

It can be seen from Fig.17 that when the blade chord height  $h$  is 78mm, the head  $H$  of the tool is 3.3m. When the blade

chord height  $h$  increases to 88 mm, the head  $H$  of the tool decreases to 3.0m. When the blade chord height  $h$  continues

to increase to 98mm and 108mm, the head  $H$  of the tool stabilizes to 3.0m. With the increase of the blade chord height  $h$ , the head  $H$  generated by the tool decreases first and then the head  $H$  of the tool tends to be stable with the continuous increase of the blade chord height  $h$ . When the blade chord height  $h$  is 78 mm, the head  $H$  is reduced by 12% compared with that when the blade wall thickness  $b$  is 88mm. This is because the blade chord height  $h$  increases, and the volume and force area of the blade increase. The friction energy loss will also increase, so when the blade chord height  $h$  increases, the head  $H$  of the tool will decrease, but the increase of the blade chord height  $h$  can better convert the circumferential motion of the fluid into an axial motion, which has a strong stabilizing effect on the fluid. Therefore, the head  $H$  of the tool tends to be stable after the blade chord height  $h$  is 88 mm. It can be seen from Fig.18 that when the blade chord height  $h$  is 78mm, the efficiency  $\eta$  of the tool is 70%. When the blade chord height  $h$  increases to 88mm, the efficiency  $\eta$  of the tool increases to 81%. When the blade chord height  $h$  continues to increase to 98mm, the efficiency  $\eta$  of the tool increases to 83%, and the blade chord height  $h$  increases to 108mm. The efficiency  $\eta$  of the tool increases to 84%. With the increase of the blade chord height  $h$ , the efficiency  $\eta$  of the tool also increases. When the blade chord height  $h$  is 78mm, the efficiency  $\eta$  is increased by 20% compared with the efficiency  $\eta$  when the blade chord height  $h$  is 108mm. Although there is a change, this is because the increase of the blade chord height  $h$  inhibits the generation and development of the secondary backflow in the fluid flow field, and can better convert the circumferential motion of the fluid into axial motion, which has a strong effect on the steady flow of the fluid. Therefore, the efficiency  $\eta$  of the tool increases with the increase of the blade chord height  $h$ .

## 5. Conclusion

In this paper, based on the principle of eddy current, a numerical model of the vane pump annular pressure reducing downhole tool is established. The influence of different structural parameters on the head and efficiency of the tool is discussed. The following conclusions are obtained.

[1]. The range of structural parameters of the annular pressure-reducing downhole tool in a vane pump has a significant influence on the generated head  $H$ . Specifically, an increase in the number of blades ( $n$ ) results in an elevation of head  $H$ . Moreover, the blade outlet angle ( $\alpha$ ) initially rises and then declines until it reaches a certain value with increasing blade wall thickness ( $b$ ) and blade chord height ( $h$ ). Consequently, variations in blade wall thickness  $b$  and blade chord height  $h$  no longer exhibit sensitivity towards affecting

the head  $H$ .

[2].The efficiency of the downhole tool, specifically the vane pump annular pressure downhole tool, is influenced by changes in its structural parameters. The number of blades ( $n$ ) positively affects efficiency, while an increase in the chord height ( $h$ ) and blade exit angle ( $\alpha$ ) negatively impact efficiency. Initially, changes in the blade exit angle ( $\alpha$ ) have little effect on efficiency; however, as it increases along with the blade wall thickness ( $B$ ), there is a decrease in efficiency. Additionally, there is a slight decrease in tool efficiency with an increase in blade wall thickness ( $B$ ), although this parameter has minimal sensitivity.

[3].The head generated by the downhole tool of the vane pump annular airborne pressure is maximized when it has 8 blades, a blade outlet [1-7]angle of 30°, a blade chord height ( $h$ ) of 78mm, and a blade wall thickness ( $b$ ) of 25mm. Similarly, the efficiency of the vane pump annular pressure downhole tool is maximized when it also has 8 blades but with a modified blade outlet angle of 25°, an increased blade chord height ( $h$ ) to 108mm, and the same blade wall thickness ( $b$ ) of 25mm.

## References

- [1] Rivlin, R.S., Large elastic deformations of isotropic materials. I. Fundamental concepts. Philosophical transactions of the Royal Society of London. Series A: Mathematical and physical sciences, 1948. 240(822): p. 459-490.
- [2] Litvinenko, V. and M. Dvoynikov, Methodology for determining the parameters of drilling mode for directional straight sections of well using screw downhole motors. Journal of Mining Institute, 2020. 241: p. 105.
- [3] Biletskyi, V., S. Landar and Y. Mishchuk, Modeling of the power section of downhole screw motors. Mining of Mineral Deposits, 2017. 11(3): p. 15-22.
- [4] Wu, H., et al., Numerical and experimental investigation into failure of T700/bismaleimide composite T-joints under tensile loading. Composite Structures, 2015. 130: p. 63-74.
- [5] Alfano, G., On the influence of the shape of the interface law on the application of cohesive-zone models. Composites Science and Technology, 2006. 66(6): p. 723-730.
- [6] Liagov, I., A. Liagov and A. Liagova, Optimization of the Configuration of the Power Sections of Special Small-Sized Positive Displacement Motors for Deep-Penetrating Perforation Using the Technical System "Perfobore". Applied Sciences, 2021. 11(11): p. 4977.
- [7] Saeedifar, M., et al., Prediction of delamination growth in laminated composites using acoustic emission and Cohesive Zone Modeling techniques. Composite Structures, 2015. 124: p. 120-127.